

Application of Improved Chameleon Swarm Algorithm and Improved Convolution Neural Network in Diagnosis of Skin Cancer

Wu Beibei, Sanquan College of Xinxiang Medical University, China*

Nikolaj Jade, University of Wrocław, Poland

ABSTRACT

Skin cancer is affected by the uncommon evolution of skin cells and is a deadly type of cancer. In addition, skin lesion is affected by numerous factors, such as exposure to the sun, infections, allergies, etc. These skin illnesses have become a challenge in therapeutic diagnosis because of virtual resemblances, where image classification is vital to sufficiently diagnose dissimilar lesions. Therefore, early diagnosis is significant and can avert skin cancers like focal cell carcinoma and melanoma. A deep learning-based computer analyzing model can be an automatic solution in medical evaluations to overcome this issue. Hence, this paper suggests an improved chameleon swarm algorithm and convolutional neural networks (ICSA-CNN) for effective skin cancer identification and classification. The data are collected from the Kaggle dataset for classifying skin cancer. Chameleon swarm algorithm is a clustering technique utilized in data mining to the cluster dataset utilizing dynamic systems, and it can resolve constrained and global numerical optimization issues in skin cancer detection.

KEYWORDS

Chameleon Swarm Algorithm, Classification, Convolutional Neural Networks, Skin Cancer, Skin Lesions

INTRODUCTION

A significant rise in deaths may be attributed to a lack of awareness about the warning signs of skin cancer and how it can be prevented. Skin cancer is regarded as one of the most toxic forms of cancer (Kadampur et al., 2020). Exposure to UV rays from the sun is a major risk factor for developing skin cancer (Vijayalakshmi, 2019). Possible causes of cancer include sun exposure, weakened immune systems, genetic predisposition, and other factors (Nahata & Singh, 2020). Benign and malignant conditions may exhibit this erratic cellular development pattern. The term “mole” is often used to refer to benign tumors, a subset of malignancy (Amin et al., 2020). Malignant tumors, on the other hand, are considered cancer and are aggressively treated. They pose a risk to the body’s other tissues (Kumar et al., 2020). The skin’s outer layer comprises three distinct cell types: basal cells, squamous cells, and melanocytes (Goyal et al., 2020). These cells are responsible for the tissues becoming cancerous. Different skin cancers are considered dangerous; they include basal cell carcinoma (BCC),

DOI: 10.4018/IJDWM.325059

*Corresponding Author

This article published as an Open Access article distributed under the terms of the Creative Commons Attribution License (<http://creativecommons.org/licenses/by/4.0/>) which permits unrestricted use, distribution, and production in any medium, provided the author of the original work and original publication source are properly credited.

squamous cell carcinoma (SCC), and melanoma (Ashraf et al., 2020). Initially, cancer cells appear as flat patches in the skin, often with scaly, rough, reddish, or brown surfaces (Adegun, 2020). A huge brown area with darker specks is a sign of skin cancer. Other signs are a mole that mutates in appearance, whether in size, texture, or blood supply; a small lesion with an uneven border and varying shades of color; or an itchy or burning sore that causes discomfort (Togacar et al., 2021). Therefore, early detection is crucial in treating skin cancer. To diagnose skin cancer, doctors often do a biopsy. New skin patches or existing patches that change in size, shape, or color warrant a medical evaluation. Skin cancer can develop from any abnormality in the skin, including a sore, tumor, blemish, marking, or change in the skin's appearance or texture. This treatment aims to get a tissue sample from a suspicious skin lesion to evaluate its malignant potential. The procedure is tedious, lengthy, and time-consuming (Khan et al., 2021).

In the current diagnostic system, image processing techniques are commonly employed to bring illness identification methods into remote treatment (Khan et al., 2019). Image processing techniques use one or multiple computer fusion models to examine melanoma and suspected lesions (Jinnai et al., 2020). To make this handcrafted imaging method fully automatic and more intelligent, academics implement deep learning (DL) models, where an extensive data set of skin lesion images is used for testing and training the multilayer neural network (Adegun, 2021). As a result, computer-based technology delivers a less expensive, more comfortable, and early diagnosis of skin cancer signs (Rehman et al., 2020). One of the best methods to accurately and swiftly identify skin cancer is using DL (Saba et al., 2019). Human diseases, treatments, symptoms, signs, and aberrant investigation findings are all cataloged and linked together in a diseases database. Hence, the database decides which pictures to identify with which diseases based on findings.

Recently, convolutional neural network (CNN) technology has been extensively used in medicinal image processing, particularly for therapeutic image segmentation (Wei et al., 2020). These CNN-based approaches can be categorized by pixels to differentiate background substances from foreground substances to attain the last segmentation (Fraivan et al., 2022). The chameleon swarm algorithm (CSA) is a recently devised metaheuristic algorithm inspired by chameleons' intellectual behavior in nature (Malibari et al., 2022). CSA is a bottom-up clustering technique used in data mining to cluster databases using dynamic models; CSA can resolve both constrained and global numerical optimization issues (Thurnhofer-Hemsi & Dominguez, 2021). The CSA performance is evaluated using the database containing real-world applications (skin cancer diagnosis) for feature selections (Ali et al., 2022).

This paper includes three major contributions:

- Designing the ICSA-CNN model for effective skin cancer prediction and classification.
- Introducing the improved CSA and assessing the mathematical models of CNN for classifying the skin lesions from the data set.
- Showing how after the numerical outcomes have been implemented, the suggested ICSA-CNN model increases the accuracy, F1 score, sensitivity, and specificity compared with other popular models.

In the remainder of the paper we discuss the related works, propose the ICSA-CNN model, explain how we attained the numerical outcomes, and share our conclusion.

RELATED WORKS ON SKIN CANCER DETECTION

Khamparia et al. (2021) suggested an internet of health things-driven DL framework (IoHT-DLF) for detecting and classifying skin tumors. The suggested framework uses fully connected layers of a CNN to classify malignant and benign skin cells using max pooling and dense operation. These features

are retrieved automatically from pictures using several pretrained architectures, such as VGG19, SqueezeNet, Inception V3, and ResNet50. Thus, the proposed framework successfully detects and classes skin cancer from photos of skin lesions, achieving high precision, recall, and accuracy levels.

Alfi et al. (2022) proposed DL ensemble stacking of the machine learning (ML) model (DLESMLM) for diagnosing melanoma skin cancer. These researchers explained how they trained initial ML models using manually created features, such as random forest (RF), support vector machine (SVM), gradient boosting machine (GBM), logistic regression (LR), and K-nearest neighbor (KNN), and then hypothesized how these foundational models are able to train levels using one model stacking by cross-validations on training sets. DL methods pretrained on ImageNet data have been used for transfer learning (for example, Xception, MobileNet, ResNet50V2, ResNet50, and DenseNet121). The optimum model for categorizing skin lesions was determined by calculating the F1 score, accuracy, Cohen's kappa, receiver operating characteristic (ROC) curves, and confusion matrices.

Alom et al. (2019) recommended the Inception Recurrent Residual Convolutional Network (IRRCN) for skin tumor segmentation and classification. First, this model guarantees superior feature representation for semantic segmentation by combining low- and high-level feature maps. Second, using the same or fewer network parameters, this network achieves higher quality and quantitative outcomes than competing approaches. Third, compared with the Recurrent Residual U-Net (R2U-Net), the experimental findings reveal that it performs better on segmentation tasks. In conclusion, the International Skin Imaging Collaboration (ISIC) 2018 data set dermoscopy testing accuracy reveals that the classification model achieves about 87%.

Thanh et al. (2020) discussed the adaptive principal curvature, color normalization, and feature extraction (APC-CN-FE) for skin cancer detection. The procedure has three steps: adaptive principal curvature for preprocessing skin lesion pictures, color normalization for segmenting skin lesions, and the ABCD (asymmetry, border, color, diameter) rule for feature extraction (Thanh et al., 2020). According to Thanh et al. (2020), melanoma skin cancer recognition results show that the suggested technique has great accuracy and better performance. For example, these researchers showed that the Sorensen-Dice, accuracy, and Jaccard scores for the segmentation phase were 93.9%, 96.6%, and 88.7%, respectively, and were up to 100% for the melanoma, detection phase using the ISIC data set.

Khan et al. (2021) described the EfficientNet and Extreme Gradient Boosting (EN-XGB) model for detecting skin tumors; these researchers used the EfficientNet DL model to analyze skin lesions, and XGB for medical data inside an ensemble-learning framework. They included six dissimilar categories of skin tumors in the PAD-UFES-20 data set used for the research. Khan et al. (2021) showed that with an accurateness of 0.78, a recall of 0.86, a precision of 0.89, and an F1 score of 0.88 for the PAD-UFES-20 database, the suggested model exceeded the results attained by a prior study.

Bi et al. (2021) considered the metaheuristic algorithm combined with SVM (MHA-SVM) for computer-assisted skin tumor diagnosis. First, these researchers employed feature extraction based on 20 dissimilar features after performing preprocessing procedures, such as contrast enhancement, picture thresholding, and mathematical morphology, to emphasize the crucial regions. They then used a refined version of the world cup optimization technique for feature pruning to simplify the system. Once the characteristics were optimally selected, they were fed into an SVM classifier to identify the malignant regions. Bi et al. (2021) shared that the proposed technique achieved an accurate detection rate of 92.64% for American Chemical Society (ACS) photos, and for ISIC images, it achieved a rate of 87.5%. Furthermore, Bi et al. (2021) showed that the false acceptance and rejection rates were lower than 4.41% and 9% for ACS and ISIC images, respectively.

Based on our survey of published research, we found several issues with existing methods in achieving high accuracy, sensitivity, specificity, and F1 score, such as IoHT-DLF, DLESMLM, IRRCN, APC-CN-FE, EN-XGB, and MHA-SVM. Hence, this article presents an ICSA-CNN skin cancer identification model designed to improve the classification accuracy, sensitivity, specificity, and F1 score.

ICSA-CNN

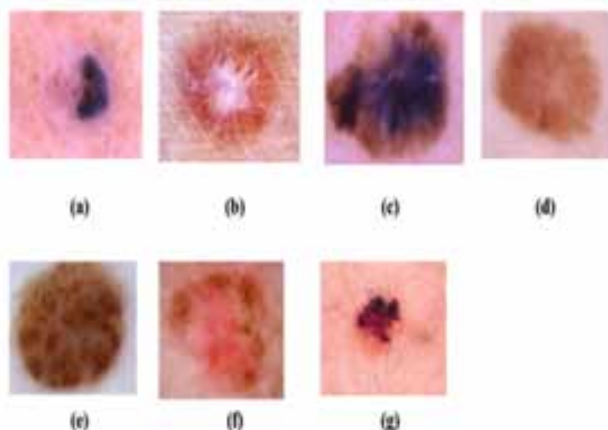
Melanoma of the skin is the most frequently occurring malignant tumor worldwide. Uncontrolled cell division leads to the development of cancer. The UV radiation in natural sunshine and tanning beds may alter the DNA in the nucleus of skin cells. Skin cancer begins as a fast-growing mole that bleeds, a tumor, or a wound that does not heal if the immune system cannot fix the damage. If ignored, it may spread to other body parts (metastasis). Melanoma is a serious skin cancer. It is significant to note that melanoma is the most lethal form of skin cancer. In most cases, melanoma starts as a change in an otherwise healthy mole or the appearance of a new, large, dark brown or black spot on the skin. As a result, making a prompt diagnosis is crucial to effectively treat the disease. We propose identifying and classifying skin cancers more effectively with the help of an enhanced version of the ICSA-CNN.

If the condition is not detected in time, the lesion might spread under the skin, making treatment more difficult. Recently, with the prompt development of DL, the classification and segmentation technique based on CNN has been first applied in image classification and achieved significant results in skin lesion classification. Hence, this article suggests an ICSA-CNN model for skin cancer prediction and diagnosis. This study presents metaheuristic algorithms named CSA for resolving global numerical optimization issues. The chameleons in the proposed method explore the whole search space looking for diseased tissue. With their large, round eyes, chameleons can see a large area around them, allowing them to search more thoroughly. In addition, they use their abnormally lengthy and sticky spots to swiftly take up damaged cells with remarkable efficiency. We suggest the use of an adaptive parameter throughout iterations of CSA to further comprehend a balance between exploitation and exploration for more consistent performance to help chameleons better search in search spaces.

Figure 1 shows the sample skin images of different classes. (Note: We used a public database in this experiment in trained CNN models.)

In this study we validated and trained CNN models using a public database of images containing seven categories of skin lesions: basal cell carcinoma (BCC), dermatofibroma (DF), actinic keratoses (AKIEC), benign keratosis lesions (BKL), melanoma (MEL), vascular lesions (VASC), and melanocytic nevi (NV). We acquired dermoscopic lesion images from ISIC and the Kaggle data set. A disease label for every photo was identified diagnostically or histopathologically. A training database for classification contained seven images (BCC, AKIEC, BKL, MEL, DF, VASC, and NV samples) with the corresponding disease labels (ground truths), validation sets, and a test set of images without ground truth, respectively. The seven different types of skin lesions represented in

Figure 1. Sample skin images of different classes



the image database used in this analysis are shown in Figure 1 and are as follows: (a) BCC, (b) DF, (c) MEL, (d) NV, (e) AKIEC, (f) BKL, (g) VASC.

Cancer that begins in the lower epidermis and develops into round cells is BCC. This cell type is responsible for around 80% of all cases of skin cancer. The term “ground truth” is used to describe the actual state of the problem that an ML model is attempting to solve. A training database does the labeling of the training photos. Data scientists can assess the accuracy of the model’s predictions on unseen data by comparing them with the validation data. Although every data scientist does not use validation data, we believe this data might be useful for optimizing hyperparameters that affect how the model evaluates data. This step is done for the purpose of classification of images with labels.

Although a BCC may occur anywhere on the skin, it most often appears on the face and neck. Children who get radiation treatment are at a higher risk, and sun exposure is a major factor. Most cases of this type of skin cancer progress slowly and do not metastasize. Sunburn and other forms of skin damage are typical causes of skin lesions. Sometimes they’re an indicator of something more serious, such as an infection or an autoimmune disorder. Although most skin lesions are completely benign, others may indicate more dangerous conditions.

Most cases of skin conditions known as dermatofibroma occur deep inside the dermis. DFs, often known as superficial/cutaneous benign fibrous histiocytomas or common fibrous histiocytomas, are a type of benign fibrous histiocytoma.

Melanoma cells, often known as melanocytes, cluster around the skin’s interface with the dermis. Melanocytes are responsible for skin color because they generate the pigment melanin. The most lethal form of skin cancer, known as melanoma, begins in cells called melanocytes. It’s responsible for around 1% of all cases of skin cancer.

A giant congenital melanocytic nevus is an excessively dark, noncancerous skin patch (nevus) consisting of pigment-generating cells termed melanocytes. It is either shown at or shortly after birth, making it congenital. If correctly identified, melanocytic nevi are fully physiologically stable and harmless lesions. Yet melanocytic nevi are often encountered with malignant melanomas.

Damaged skin from the sun and/or indoor tanning often develops a precancerous condition called actinic keratosis (AKIEC). This issue is often known as solar keratosis. Tiny areas of skin that are abnormally dry, scaly, or crusty are frequently the first indicators of AKs. In addition to varying color and elevation, these areas may also be light, red, dark brown, white, flesh-toned, pink, or a mix of these. Actinic keratoses have a rough appearance and texture, making them more noticeable to the touch than to the eye.

Benign keratoses (BKI), often known as seborrheic keratoses, appear on the skin and look like tumors. All these tumors have been ruled out as malignant. If an inflamed seborrheic keratosis has become red and inflamed, it could be easily mistaken for a nevus.

Vascular lesions, more often known as birthmarks, are a frequent type of subcutaneous and skin tissue abnormality. Vascular lesions may be broken down into three broad groups: diseases such as hemangiomas, vascular malformations, and pyogenic granulomas.

For this study we collected data from Kaggle [27] and ISIC [28] data sets for detecting skin cancer and classification. Given an image $Y = \{y_j\}_{j=1}^M, y_j \in [0, 255]^3$ belonging to D class, the convolutional networks carry out a set of operations to identify which classes $l \in \{1, \dots, D\}$, the image falls. These processes can be signified as functions as shown in equation (1):

$$\mathcal{F}(Y, S) = \arg \max_l x_l \tag{1}$$

As shown in equation (1), S signifies the variables of the trained neural networks and x_l are the class likelihoods formed by the net. For this study the image represented here as functions is shown in equation (2):

$$\mathcal{F}(Y, S) = \arg \max_i x_i \tag{2}$$

In equation (2) S represents the parameters within the neural networks under study, and x_i are the probabilities assigned to classes by the neural network.

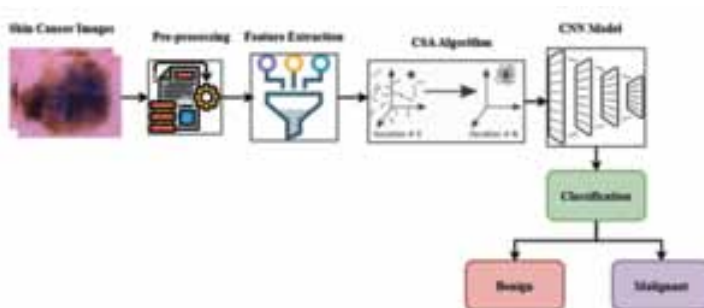
Figure 2 shows the proposed ICSEA-CNN model. We provide a preprocessing method to augment and facilitate learning our suggested classification technique from training data sets. In this paper we used a CNN to establish melanoma dermoscopic images' feature extraction. We trained a pretrained model of a CNN on databases that consist of numerous images of various classes. According to ML tasks, feature extraction was used to improve picture classification outcomes.

A CNN is a special form of network design for DL algorithms that is employed in image recognition and other pixel-based applications. Although DL employs a wide variety of neural networks, CNNs are the preferred network architecture for tasks such as object recognition and identification.

CNNs use pooling and convolution layers to extract the necessary features automatically during the training stage. The use of feature selection for practical applications in the medical sciences has increased dramatically, allowing professionals to make informed decisions. In contrast, traditional algorithms converge slowly to a solution to the feature selection issue and tend to become stopped in specific contexts. Therefore, we were motivated to suggest an improved feature selection technique by combining CSA with CNN. Chameleons are a unique species that can change color according to their surrounding environment. Improved prediction models that classify skin lesions into malignant or benign lesions are based on a new regularizer method. A benign growth is noncancerous, typically develops slowly, and doesn't spread to other body parts. A malignant growth, on the other hand, is cancerous, can overgrow, and, in some cases, can spread to tissues in other parts of the body.

Regarding CNNs, the decision of whether or not to activate a neuron is made by an activation function. Thus, a CNN will use more elementary arithmetic to determine whether the neuron's input to the network is relevant to the prediction process. Rectified linear unit (ReLU) has seen the most use in this research, and it is defined in the actual picture. Hence, using ReLU helps to avoid the need for an ever-increasing amount of computing to run the neural network. Adding more ReLUs increases the computational cost linearly as the size of the CNN grows. By introducing nonlinearity into a DL network, activation functions such as the ReLU can avoid the problem of vanishing gradients. The upbeat side of its argument is explained. It is often used in DL as an activation function. Training neural networks involves iteratively finding parameter values (model weights) that minimize error or loss when applied to the training data set. ReLU's activation threshold still introduces nonlinearity even if the pixel values are scaled between 0 and 1. Backpropagation fails to update the weights when the majority of these neurons provide zero as an output. In the end, much of the network stops working,

Figure 2. Proposed ICSEA-CNN model



rendering it incapable of acquiring any new knowledge. Because the derivative of the ReLU function is 0 for all negative inputs, it cannot be differentiated, despite its continuous nature. ReLU's output is useful for gradient descent because it is not saturated, and therefore, it has no upper bound on its value.

Activation functions are used for every neuron, which is often a ReLU, with functions $f(y) = \max(y, 0)$. This procedure is established on the actual picture. ReLU is the activation layers in the convolutional neural network to improve the training phase on the neural network that has the benefit of minimizing mistakes. ReLU activation creates every pixel value 0 when a pixel image has a value of < 0 . Every input component is subjected to threshold operations by ReLU functions $f(y)$, with any value less than 0 equal to 1. This process is the same as the one shown in equation (3):

$$f(y) = \begin{cases} y, & y \geq 0 \\ 0, & y < 0 \end{cases} \quad (3)$$

Max pooling, a procedure that sends only maximum values to the next layers of sliding grids, has been used to scale down the output. After a CNN has been constructed, an optimization approach based on its internal weights is needed so that it may be tailored to a specific task. The gradient descents rely on reducing the cross-entropy losses as fitness functions as shown in equation (4):

$$K = \sum_{i=1}^M \sum_{j=1}^N -c_i^{(j)} \log z_i^{(j)} \quad (4)$$

As inferred from equation (4), $c_i^{(j)}$ defines desired output vectors, and $z_i^{(j)}$ denotes acquired output vectors of the n^{th} class. Softmax functions are demonstrated in the subsequent formulation shown in equation 5:

$$z_i^{(j)} = \frac{e^{f_i}}{\sum_{j=1}^N e^{f_i}} \quad (5)$$

In equation (5), N denotes the number of samples.

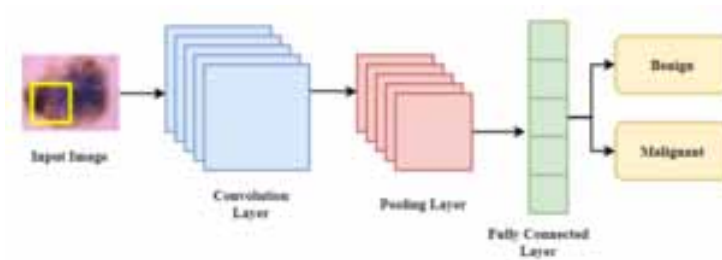
The K function can be reformed by weights penalty to comprise δ values to keep the value of the weight from receiving higher as shown in equation (6):

$$K = \sum_{i=1}^M \sum_{j=1}^N -c_i^{(j)} \log z_i^{(j)} + \frac{1}{2} \delta \sum_L \sum_K S_{l,k}^2 \quad (6)$$

In equation (6), S_l defines connection weights, l is the layer, and K and L are the overall number of layers and layers k connection, respectively.

Figure 3 shows the CNN model. Several dynamic filters are trained in the convolution layer according to classification tasks during the training stage. Likewise, pooling layers downsample the surrounding pixels into a single pixel while retaining the shape and size of the invariant feature. Convolution layers are used to assess the output of neurons coupled to a local region at the input. Point multiplication between neuron weights and the regions to which they are linked does the computation (the activation weight). The pooling layers are used to subsample the input picture to lessen the required

Figure 3. CNN model for skin cancer classification



processing time, amount of storage space, and complexity of the network's parameters (overfitting). Decreasing the input size input picture results in CNNs being less affected by the displacement of the input image (independent of the position). The classification system includes seven categories. The pretreatment method is used to assign items to these categories.

We found a mathematical model in the feature selection phase for the tasks that CNNs are carried out. A biopsy is the gold standard for determining the presence of skin cancer. A skin biopsy is the method your dermatologist will use to get rid of the area. A skin biopsy is a necessary procedure. It's the only surefire approach to detect skin cancer in its early stages. If a neural network has convolutional layers, it is said to be convolutional. CNNs take their cues from the visual cortex system found in humans and other animals, whereas general neural networks take their cues from the human brain more broadly. Because not all input nodes are responsible for all output nodes, convolutions are not densely connected; therefore, these nodes allow for greater adaptability in learning by convolutional layers. When dealing with high-dimensional inputs such as image data, the reduced number of weights per layer is especially helpful. CNN models may analyze an image of a human body part, such as the lungs, to determine the likely location of a tumor or other anomalies, such as fractured bones in X-ray scans, based on the network's history of processing similar images. Likewise, medical imaging studies such as computerized tomography (CT) scans and mammograms can aid in the detection and diagnosis of cancer.

The inputs are modified by adding weights to them as they travel via the synapses to the cell. The "sum of weighted inputs" from each incoming synapse is then processed by an activation function and sent on to all neurons in the following layer. An activation function is a piece of code included into a neural network simulator to improve the network's ability to recognize and learn from complex input patterns. In a similar vein to how our brains work, the activation function ultimately determines which neuron will fire.

During the building of a CNN, the convolutional layer(s) are followed by a pooling layer that calculates the maximum or average of the input and then downsamples it using the information from the convolutional layers. In CNN, a pooling or subsampling layer typically comes right after a convolution layer. Its purpose is to reduce the resolution of a convolution layer's output in two spatial dimensions. As the size of the input picture is reduced, the effect of image displacement on CNNs is reduced.

When a model is overfit, it matches the training data too well. When this happens, the model has a hard time extrapolating to data that wasn't included in the training set. For instance, instead of recognizing broad patterns, your model is adept at recognizing individual photos from your training set.

Training times for a CNN model can be decreased, efficiency can be improved, and overfitting can be avoided by using pooling layers. Although the max pooling layer emphasizes the most striking parts of an image, the average pooling layer softens it while still preserving its essential details.

In a binary step activation function, the threshold value decides whether a neuron is activated. The input value is compared with a predetermined threshold by the activation function. The neuron becomes active if—and only if—the input value is larger than the activation threshold.

The non-linearities made possible by various activation functions may lend themselves more effectively to the solution of some functions than others. The ReLU function's primary benefit over competing activation functions is that it does not simultaneously activate all of the neurons. The problem with ReLU is that it can't learn from data where the activation value is 0. When the hidden layers are programmed with ReLU and the entire network is initialized with 0, this is the typical result. Hence, in recent years, the vast majority of skin cancer classification challenges have been successfully resolved using DL-based methods such as CNN.

CSA is population-based algorithms and d -dimensional search space. Every chameleon denotes solutions to an issue, so if m candidate is the solution, the $m \times d$ dimensional two-dimensional x matrices can be described as chameleon populations in skin cancer diagnosis, as shown in equation (7):

$$x_t^j = [x_{t,1}^j, x_{t,2}^j, \dots, x_{t,d}^j] \quad (7)$$

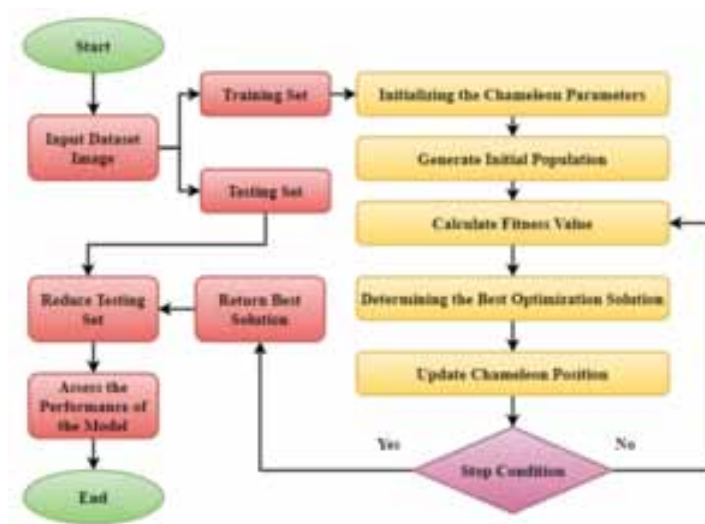
As inferred from equation (7), $j = 1, 2, 3, \dots, m$ and t are valid iteration, and $x_{t,d}^j$ signifies the position in the d^{th} dimension.

Figure 4 shows the process of the CSA for feature selection. The main objective of using CSA is to enhance the capability to balance exploration and exploitation while searching for a feasible solution. The random mathematical values for M chameleons are then assigned, and fitness values for every patient are computed. Then, the patient with the best fitness value is used as the best chameleon. The solution is then changed using Cham exploitation. The last step is updating individuals until the stop criteria are met. Then, based on the best solution, the testing set's size is decreased, and the implemented CSA as feature selection is assessed by several metrics.

The statistical model of positions updates of chameleons' movements and behavior while examining for skin lesions could be provided by the formula shown in equation (8):

$$x_{t+1}^{j,i} = \begin{cases} x_t^{j,i} + q_1(Q_t^{j,i} - H_t^i)r_2 + q_2(H_t^i - x_t^{j,i}) & r_1 r_j \geq Q_q \\ x_t^{j,i} + \mu((v^i - k^i)r_3 + k_a^i) \text{sgn}(\text{rand} - 0.5) & r_j < Q_q \end{cases} \quad (8)$$

Figure 4. Process of the CSA for feature selection



As shown in equation (8), $x_{t+1}^{j,i}$ indicates new positions of the j^{th} chameleon in the i^{th} dimensions in the iterations stage. $Q_t^{j,i}$ signifies best positions occupied by the i^{th} size chameleons in the t^{th} iterations loop. $x_t^{j,i}$ denotes the current positions of the chameleon, and H_t^i denotes global best positions. r_1 , r_2 , and r_3 denote the arbitrary numbers evenly spaced from 0 to 1. q_1 and q_2 indicate the two positive numbers that control exploratory capability. μ is a variable described as functions of reducing iteration. Q_q denotes the chameleon's likelihood of identifying affected cells. r_j indicates the uniformly produced arbitrary number in the indices j among 0 and 1. $\text{sgn}(\text{rand}-0.5)$ has an effect on exploration directions and can be -1 or 1 . The suggested ICSA-CNN model enhances the classification accurateness, specificity, sensitivity, and F1 score better than other popular methods.

The primary goal of using CSA is to enhance one's capacity to balance both discovery and extraction while solution hunting. $q1$ and $q2$ denote the two integers that govern the scope of exploration and represent the chameleon's propensity to recognize diseased cells.

μ changes over the course of the algorithm where it is a parameter defined in terms of functions that optimize repetition.

Qq indicates how well the chameleon can detect diseased tissue. rj represents the evenly generated random number between 0 and 1 for index j . The cancer types can be accurately and sensitively identified by the artificial intelligence technique. ML is well suited to the task of parsing the variations in gene expression among cancers of an unknown source.

For the neural convolutional map for CNN to function, it must first receive an image, assign a value to each object in the picture, and then separate those objects from one another. When compared with other DL-based methods, CNN requires minimal preprocessing of data.

The earlier cancer is detected, the better the chances of survival. Knowing what to look for on your own skin can help you catch cancer in its earliest, most treatable stages, before it causes any harm or disfigurement or even death.

A system for assessing skin photographs for the purpose of diagnosing skin cancer can be developed with the use of deep CNNs. To treat skin cancer successfully and improve patient outcomes, early detection is essential.

Our goal is to use a CNN to develop a model that can both detect and categorize different types of skin cancer. Our approach involves training a CNN on the ICSA data set of pictures to detect and diagnose skin cancer. When applied to a data set of known benign and cancerous samples, the suggested model achieves an accuracy maximum.

RESULTS AND DISCUSSION

The paper presents the ICSA-CNN model for skin cancer prediction and classification. The data were collected from the data set of Kaggle data set [27]. This data set consists of a balanced data set of malignant and benign skin moles images. The data consist of two folders with 1,800 pictures (224 x 244) of the two categories of moles. All images have been organized consistent with the classification taken with ISIC, and all subsets have been separated into the same number of images except moles and melanomas, whose images are slightly dominant. A historical sample of patients presenting for skin tumor screening at many institutions provided photos of lesions obtained with different dermatoscopy types from every anatomic location (excluding nails and mucosa). There is only ever one main lesion shown in a given image of a lesion; any additional fiducial markers, subsequent lesions, or areas of pigmentation are ignored. The performance of the suggested ICSA-CNN model has been executed based on the metrics such as classification accuracy, specificity, sensitivity, and F1 score. In this experiment, CNN using loss functions classified extracted features into four groups: dark circles, acne, spots, and blackheads.

Classification Accuracy Ratio

Automated methods of skin cancer detection using image processing would greatly assist dermatologists and improve diagnostic accuracy. Consequently, improved melanoma identification can help patients demonstrate indicators of the illness. Furthermore, a CNN can learn from features hierarchically. As a result, CSA can be regarded as a precise and efficient optimization method for undertaking the feature selection issue because it can determine the feasible areas that consist of viable solutions, as perceived from the quality of the chosen feature that impacts the classification accurateness. Several feature selection issues (such as the real-time application of skin cancer detection) are tested in experiments and analyzed regarding the fitness function, classification accuracy, and the number of chosen features. Figure 5 demonstrates the classification accuracy of the recommended ICSA-CNN model:

$$Accuracy = \frac{TP + TN}{TP + FP + TN + FN} \quad (9)$$

In equation (9), TP denotes true positives, TN indicates true negatives, FP represents false positives, and FN signifies false negatives.

F1-Score Ratio

The F1 score is a common statistic used to calculate the quality of a DL model. It combines a model's accuracy with its reliability. A model's accuracy is measured by how often it correctly predicts a value over the full data set. Recall measures how well a model can identify every instance that belongs to a given class. Precision in the context of classification models is their capacity to selectively retrieve instances that belong to a given class. Recall and precision are combined into a score called F1 using the harmonic mean. The accuracy and F1 score delivers a general outline of the performance, considering the negative and positive samples. Figure 6 illustrates the F1-score ratio of the suggested ICSA-CNN model:

$$F1 - Score = 2 \cdot \frac{Precision \cdot Recall}{Precision + Recall} \quad (10)$$

Figure 5. Classification accuracy ratio

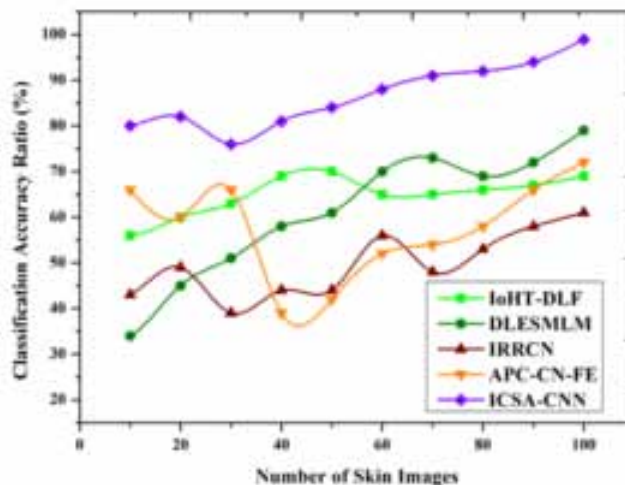
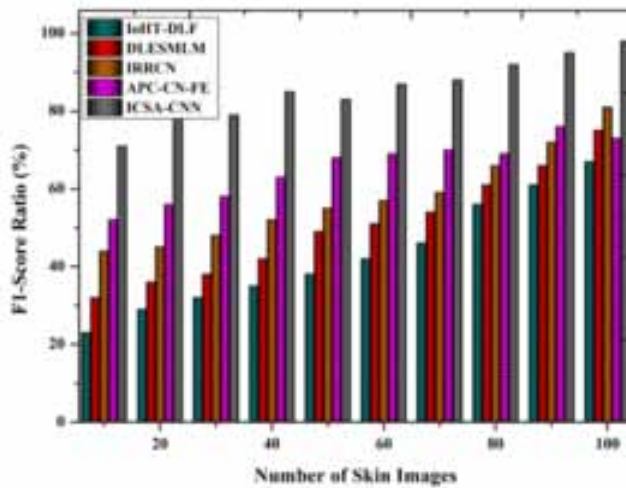


Figure 6. F1-score ratio



As inferred from equation (10), the F1-score ratio has been calculated.

Sensitivity Ratio

Skin cancer is a growing public health burden, especially melanoma. Experimental studies have indicated a potential diagnostic role for DL methods in identifying skin cancer at varying sensitivities. The specificity and sensitivity measure how well the model classifies the appropriate instances. Recall or sensitivity demonstrates the true predictive value concerning incorrectly forecast negative ailments (true positive ratio). First, this study stated the real positive cases of melanoma that have been properly forecast positive (sensitivity), the real negative cases that have been properly forecast negative (specificity), and the overall number of positive forecast cases (precision) from the confusion matrices. Figure 7 denotes the sensitivity ratio of the suggested ICSA-CNN model:

$$Sensitivity = \frac{TP}{TP + FN} \quad (11)$$

As shown in equation (11), sensitivity is calculated with true positives (TPs) and false negatives (FNs).

Specificity Ratio

If the suspicious lesions are in numerous locations, incisions for biopsy will be essential. This situation needs to evade unnecessary scarring, thereby requiring physicians to give instant, scar-free, and extremely precise (in both specificity and sensitivity) diagnoses of all types of skin cancer. Specificity is defined as the ICSA-CNN model's capability to forecast a true negative of each category available in skin cancer detection. Specificity is the ratio by which a patient is diagnosed negative during the virtual assessment that turns out to be healthy or true negative from a surgery. Figure 8 indicates the specificity ratio of the proposed ICSA-CNN model:

$$Specificity\ Ratio = \frac{TN}{TN + FP} \quad (12)$$

Figure 7. Sensitivity ratio

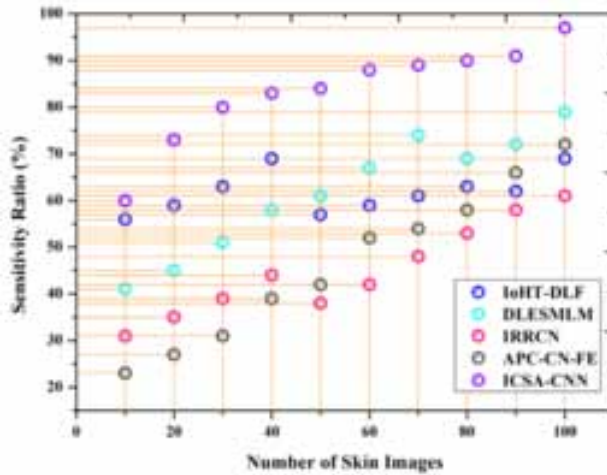
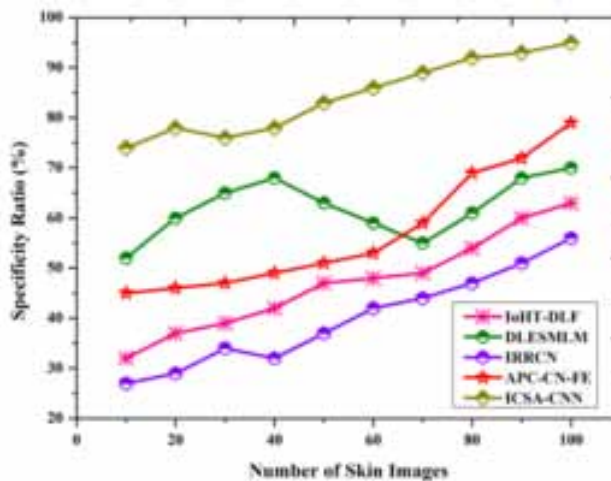


Figure 8. Specificity ratio



As shown in equation (12), specificity is calculated with TNs and FPs.

The suggested ICSA-CNN model enhances the accuracy, sensitivity, specificity, and F1 score in skin cancer detection and diagnosis compared with other existing methods, such as IoHT-DLF, DLESMLM, IRRCN, APC-CN-FE, EN-EGB, and MHA-SVM.

CONCLUSION

An effective strategy for skin lesion classification is described in light of the recent progress made in DL architectures. This study suggests the ICSA-CNN model for effective skin cancer prediction, classification, and diagnosis. This outcome showed that the CSA can select the appropriate feature and realm the classification quality. Furthermore, a deep CNN's powerful ability to learn and handcrafted features, such as color moments and texture features, are used to classify skin diseases

with high accuracy. We trained a CNN on two different skin lesion data sets, ISIC and Kaggle. Thus, the suggested model is more robust than the normal CNN classification process. The numerical outcomes prove that the suggested ICSA-CNN model improves the classification accuracy rate of 98.9%, sensitivity rate of 97.8%, specificity rate of 96.8%, and F1-score rate of 98.1% more than other popular methods. The limitation of the recommended model is that it needs to know what types of images are in each class. It might be difficult to deal with the intra-class variation because each image would need its own preprocessing. In a future study, these components will be given to a small cluster of dermatologists so that they can take images of lesions to train our DL model.

REFERENCES

- Adegun, A., & Viriri, S. (2021). Deep learning techniques for skin lesion analysis and melanoma cancer detection: A survey of state-of-the-art. *Artificial Intelligence Review*, 54(2), 811–841. doi:10.1007/s10462-020-09865-y
- Adegun, A. A., & Viriri, S. (2020). FCN-based DenseNet framework for automated detection and classification of skin lesions in dermoscopy images. *IEEE Access : Practical Innovations, Open Solutions*, 8, 150377–150396. doi:10.1109/ACCESS.2020.3016651
- Alfi, I. A., Rahman, M. M., Shorfuzzaman, M., & Nazir, A. (2022). A non-invasive interpretable diagnosis of melanoma skin cancer using deep learning and ensemble stacking of machine learning models. *Diagnostics (Basel)*, 12(3), 726. doi:10.3390/diagnostics12030726 PMID:35328279
- Ali, K., Shaikh, Z. A., Khan, A. A., & Laghari, A. A. (2022). Multiclass skin cancer classification using EfficientNets—A first step towards preventing skin cancer. *Neuroscience Informatics (Online)*, 2(4), 100034. doi:10.1016/j.neuri.2021.100034 PMID:36699194
- Alom, M. Z., Aspiras, T., Taha, T. M., & Asari, V. K. (2019). *Skin cancer segmentation and classification with NABLA-N and inception recurrent residual convolutional networks*. <https://doi.org/10.48550/arXiv.1904.11126>
- Amin, J., Sharif, A., Gul, N., Anjum, M. A., Nisar, M. W., Azam, F., & Bukhari, S. A. C. (2020). Integrated design of deep features fusion for localization and classification of skin cancer. *Pattern Recognition Letters*, 131, 63–70. doi:10.1016/j.patrec.2019.11.042
- Ashraf, R., Afzal, S., Rehman, A. U., Gul, S., Baber, J., Bakhtyar, M., Mehmood, I., Song, O.-Y., & Maqsood, M. (2020). Region-of-interest based transfer learning assisted framework for skin cancer detection. *IEEE Access : Practical Innovations, Open Solutions*, 8, 147858–147871. doi:10.1109/ACCESS.2020.3014701
- Bi, D., Zhu, D., Sheykahmad, F. R., & Qiao, M. (2021). Computer-aided skin cancer diagnosis based on a new meta-heuristic algorithm combined with support vector method. *Biomedical Signal Processing and Control*, 68, 102631. doi:10.1016/j.bspc.2021.102631
- Fanconi, C. (2019). *Skin cancer: Malignant vs. benign* [Data set]. <https://www.kaggle.com/datasets/fanconic/skin-cancer-malignant-vs-benign>
- Fraivan, M., & Faouri, E. (2022). On the automatic detection and classification of skin cancer using deep transfer learning. *Sensors (Basel)*, 22(13), 4963. doi:10.3390/s22134963 PMID:35808463
- Goyal, M., Knackstedt, T., Yan, S., & Hassanpour, S. (2020). Artificial intelligence-based image classification methods for diagnosis of skin cancer: Challenges and opportunities. *Computers in Biology and Medicine*, 127, 104065. doi:10.1016/j.combiomed.2020.104065 PMID:33246265
- Jinnai, S., Yamazaki, N., Hirano, Y., Sugawara, Y., Ohe, Y., & Hamamoto, R. (2020). The development of a skin cancer classification system for pigmented skin lesions using deep learning. *Biomolecules*, 10(8), 1123. doi:10.3390/biom10081123 PMID:32751349
- Kadampur, M. A., & Al Riyaaee, S. (2020). Skin cancer detection: Applying a deep learning based model driven architecture in the cloud for classifying dermal cell images. *Informatics in Medicine Unlocked*, 18, 100282. doi:10.1016/j.imu.2019.100282
- Katansky, A. (2019). *Skin cancer ISIC* [Data set]. <https://www.kaggle.com/datasets/nodoubttome/skin-cancer9-classesisic>
- Khamparia, A., Singh, P. K., Rani, P., Samanta, D., Khanna, A., & Bhushan, B. (2021). An internet of health things-driven deep learning framework for detection and classification of skin cancer using transfer learning. *Transactions on Emerging Telecommunications Technologies*, 32(7), e3963. doi:10.1002/ett.3963
- Khan, I. U., Aslam, N., Anwar, T., Aljameel, S. S., Ullah, M., Khan, R., Rehman, A., & Akhtar, N. (2021). Remote diagnosis and triaging model for skin cancer using EfficientNet and extreme gradient boosting. *Complexity*, 2021, 1–13. doi:10.1155/2021/5591614
- Khan, M. A., Muhammad, K., Sharif, M., Akram, T., & de Albuquerque, V. H. C. (2021). Multi-class skin lesion detection and classification via teledermatology. *IEEE Journal of Biomedical and Health Informatics*, 25(12), 4267–4275. doi:10.1109/JBHI.2021.3067789 PMID:33750716

- Khan, M. Q., Hussain, A., Rehman, S. U., Khan, U., Maqsood, M., Mehmood, K., & Khan, M. A. (2019). Classification of melanoma and nevus in digital images for diagnosis of skin cancer. *IEEE Access : Practical Innovations, Open Solutions*, 7, 90132–90144. doi:10.1109/ACCESS.2019.2926837
- Kumar, M., Alshehri, M., AlGhamdi, R., Sharma, P., & Deep, V. (2020). A de-ANN inspired skin cancer detection approach using fuzzy C-means clustering. *Mobile Networks and Applications*, 25(4), 1319–1329. doi:10.1007/s11036-020-01550-2
- Malibari, A. A., Alzahrani, J. S., Eltahir, M. M., Malik, V., Obayya, M., Al Duhayyim, M., Lira Neto, A. V., & de Albuquerque, V. H. C. (2022). Optimal deep neural network-driven computer aided diagnosis model for skin cancer. *Computers & Electrical Engineering*, 103, 108318. doi:10.1016/j.compeleceng.2022.108318
- Nahata, H., & Singh, S. P. (2020). Deep learning solutions for skin cancer detection and diagnosis. In V. Jain & J. Chatterjee (Eds.), *Machine learning with health care perspective. Learning and analytics in intelligent systems*. doi:10.1007/978-3-030-40850-3_8
- Rehman, A., Khan, M. A., Mehmood, Z., Saba, T., Sardaraz, M., & Rashid, M. (2020). Microscopic melanoma detection and classification: A framework of pixel-based fusion and multilevel features reduction. *Microscopy Research and Technique*, 83(4), 410–423. doi:10.1002/jemt.23429 PMID:31898863
- Saba, T., Khan, M. A., Rehman, A., & Marie-Sainte, S. L. (2019). Region extraction and classification of skin cancer: A heterogeneous framework of deep CNN features fusion and reduction. *Journal of Medical Systems*, 43(9), 289. doi:10.1007/s10916-019-1413-3 PMID:31327058
- Thanh, D. N. H., Prasath, V. B. S., Hieu, L. M., & Hien, N. N. (2020). Melanoma skin cancer detection method based on adaptive principal curvature, colour normalisation and feature extraction with the ABCD rule. *Journal of Digital Imaging*, 33(3), 574–585. doi:10.1007/s10278-019-00316-x PMID:31848895
- Thurnhofer-Hemsi, K., & Domínguez, E. (2021). A convolutional neural network framework for accurate skin cancer detection. *Neural Processing Letters*, 53(5), 3073–3093. doi:10.1007/s11063-020-10364-y
- Toğaçar, M., Cömert, Z., & Ergen, B. (2021). Intelligent skin cancer detection applying autoencoder, MobileNetV2 and spiking neural networks. *Chaos, Solitons, and Fractals*, 144, 110714. doi:10.1016/j.chaos.2021.110714
- Vijayalakshmi, M. M. (2019). Melanoma skin cancer detection using image processing and machine learning. *International Journal of Trend in Scientific Research and Development*, 3(4), 780–784. doi:10.31142/ijtsrd23936
- Wei, L., Ding, K., & Hu, H. (2020). Automatic skin cancer detection in dermoscopy images based on ensemble lightweight deep learning network. *IEEE Access : Practical Innovations, Open Solutions*, 8, 99633–99647. doi:10.1109/ACCESS.2020.2997710